http://dx.doi.org/10.5935/0100-4042.20150009 *Quim. Nova*, Vol. 38, No. 3, 342-350, 2015

Artigo

VIS-NIR SPECTROMETRY, SOIL PHOSPHATE EXTRACTION METHODS AND INTERACTIONS OF SOIL ATTRIBUTES

José Francirlei de Oliveira[a], Michel Brossard[b], Edemar Joaquim Corazza[c], Robélio Leandro Marchão[d], Pedro Rodolfo Siqueira Vendrame[e], Osmar Rodrigues Brito[a] and Maria de Fátima Guimarães[a,*]

[a]Departamento de Agronomia, Centro de Ciências Agrárias, Universidade Estadual de Londrina, Rodovia Celso Garcia Cid, PR 445, Km 380, 86051-980 Londrina – PR, Brasil

[b]Institut de recherche pour le développement, UMR 210 Eco&Sols, BP 64501, 34394 Montpellier cedex 5, France

[c]Embrapa Informação Tecnológica, CP 040315, 70770-901 Brasília – DF, Brasil

[d]Embrapa Cerrados, CP 08223, 73310-970 Planaltina – DF, Brasil

[e]Departamento de Geociências, Universidade Estadual de Londrina, CP 6001, 86051-990 Londrina – PR, Brasil

Recebido em 26/07/2014; aceito em 07/11/2014; publicado na web em 11/02/2015

The objective of this study was to evaluate the relationships between the spectra in the Vis-NIR range and the soil P concentrations obtained from the P_M and P_{rem} extraction methods as well as the effects of these relationships on the construction of models predicting P concentration in Oxisols. Soil samples' spectra and their P_M and P_{rem} extraction solutions were determined for the Vis-NIR region between 400 and 2500 nm. Mineralogy and/or organic matter content act as primary attributes allowing correlation of these soil phosphorus fractions with the spectra, mainly at wavelengths between 450-550, 900-1100 nm, near 1400 nm and between 2200-2300 nm. However, the regression models generated were not suitable for quantitative phosphate analysis. Solubilization of organic matter and reactions during the P_M extraction process hindered correlations between the spectra and these P soil fractions. For P_{rem},, the presence of Ca in the extractant and preferential adsorption by gibbsite and iron oxides, particularly goethite, obscured correlations with the spectra.

Keywords: Mehlich-1 extractor; remaining phosphorus; partial least squares regression.

INTRODUCTION

Traditionally, the phosphate (P) content of soil samples has been evaluated using chemical, physico-chemical and biological extraction, with limitations and advantages for each method. Historically, the application of spectroscopic techniques to the study of soils has been dedicated to mineralogical analyses.[1] However, in the last two decades, the number of studies evaluating other applications of Vis-NIR spectroscopy in soil science and agronomy has increased rapidly, with a primary focus on measuring various basic attributes of soils, such as the organic matter content, clay content and, recently, chemical attributes.[2] Between these attributes, the prediction of phosphorus in the soil through the Vis-NIR spectra have also been studied. However, the establishment of a relationship between P concentrations and Vis-NIR spectra also depends on correlations between P and other soil attributes, because when Vis-NIR method is used in combination with multivariate techniques for spectral data analysis, it has the potential to determine the chemical composition of a soil sample qualitatively or quantitatively,[3] primarily through the specific vibrations or stretching of bonds among carbon (C), hydrogen (H), nitrogen (N) and oxygen (O) present in the material.[4,5] Therefore the characterization and prediction of P using Vis-NIR spectroscopy may be possible by analyzing the bonds of this element with C, H and O, primarily in the forms P=O, P=O bonded to H, P-phenyl, P-H, P-OH and the phosphate ions (PO_3^{2-} and PO_4^{3-}), or with the C-H, C=OH, C-O, P-O and P=O bonds present in monoester or diester phosphates.[4,6,7] These correlations can be soil-specific, preventing the extrapolation of the results to other soils because the relationships between spectra and secondary attributes, such as P, are not precise and various specific interactions between these parameters need to be better understood.[7,8]

Bogrekci and Lee[9,10] Maleki *et al.*[11,12] Mouazen *et al.*[13] and Lu *et al.*[14] have demonstrated the potential of Vis-NIR spectroscopy for predicting P concentrations in soils extracted using the Olsen, ammonium lactate and Mehlich-1 methods and even for studying the spatial variability of P in soils from a temperate climate. However, Vågen *et al.*,[15] Viscarra Rossel[16] and Vendrame *et al.*[17] did not obtain good results for highly weathered soils, including latosols.

Studies that have focused on the use of spectroscopy for the prediction of Mehlich-1 P concentrations (P_M) and remaining P concentrations (P_{rem}) in the soil are scarce.[18] The P_M method, based on a double-acid extraction of forms of soil phosphate, is the most commonly used method in Brazil. The P_{rem} method is a measure of the phosphate exchange between the solid phase of the soil and a solution of calcium chloride and is derived from the classical methodology of establishing adsorption isotherms, further providing information about the phosphate buffering capacity of the sample.[19]

The P_M concentration can be indirectly correlated with the spectrum in the Vis-NIR range because of the spectral response of organic matter, given that the double acid extraction is not selective and also extracts a fraction of the P from organic matter.[20,21]

The P_{rem} concentration can also be indirectly correlated with the spectrum in the Vis-NIR range because of the spectral response of minerals from the clay fraction, given that the orthophosphate molecule establishes chemical relationships with the surfaces of the solid phase of the soil.[22] In some Brazilian soils, gibbsite represents a large fraction of the soil minerals and exhibits preferential adsorption for P relative to other anions present in the soil,[23-25] potentially aiding prediction of P concentrations. Furthermore, iron oxides and gibbsite produce active peaks in the region from 450 – 550 nm and in the region from 2200 – 2300 nm.[26-28]

The objective of this study is to evaluate the relationships between the spectra in the Vis-NIR range and the soil P concentrations obtained

*e-mail: mfatima@uel.br

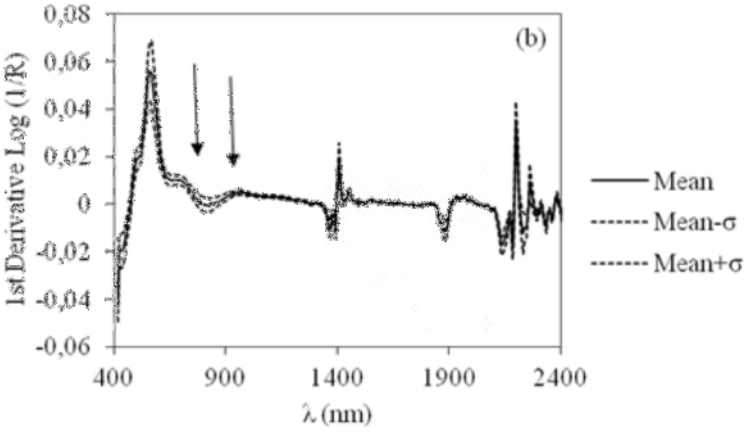

Figure 2S. *First derivative of the spectra of samples from the 11 soil profiles (n=88) used for model calibration*

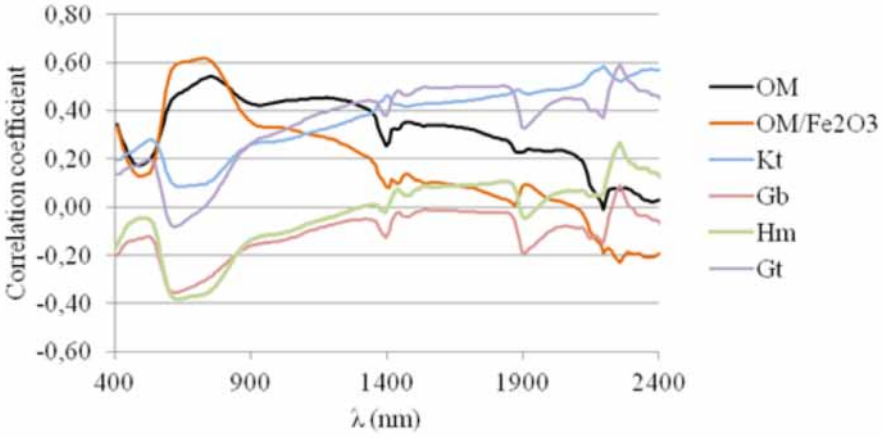

Figure 3S. *Correlation coefficients between the spectra and the organic matter to iron ratio, and the organic matter, kaolinite (Kt), gibbsite (Gb), goethite (Gt) and hematite (Hm) contents of the soil profile samples*

from the P_M and P_{rem} extraction methods as well as the effects of these relationships on the construction of models that predict the P concentration in Oxisols.

MATERIALS AND METHODS

Sampling procedure

For the study, a collection of samples from a 700-ha area of Red Yellow Latosols (according to the Brazilian taxonomic system)[29] and Red Latosols, located on the Brazilian Central Plateau (municipality of Planaltina – Goiás state) was analyzed. A description of the site is given in Oliveira *et al*..[28] A set of 88 samples was collected in triplicate from 11 soil profiles from the following layers: 0.00 – 0.05, 0.05 – 0.10, 0.125 – 0.175, 0.225 – 0.275, 0.325 – 0.375, 0.725 – 0.775, 0.875 – 0.925, 1.075 – 1.125 m. A second set of 177 samples from the 0.05 – 0.10 m layer was collected from a regular 2-ha grid.

Analytical procedure

For the general soil characterization, chemical and physical analyses were performed as described in Claessen *et al.*[30] Air-dried samples were sieved through a 2-mm mesh. The particle size analysis of the soil (air-dried fine earth) was done using the pipet method, after slow agitation for 16 hours and chemical dispersion with sodium hydroxide (NaOH, 1 mol L^{-1}).

The SiO_2, Al_2O_3 and Fe_2O_3 concentrations were obtained by extracting the soil samples with a 1:1 H_2SO_4 solution followed by inductively coupled plasma atomic emission spectroscopy (ICP-AES). The SiO_2 and Al_2O_3 concentrations were used for the calculation of kaolinite (Kt) and gibbsite (Gb) concentrations,[31] and the Fe_2O_3 concentrations were associated with the matrix and color of the soil for the calculations of the hematite (Hm) and goethite (Gt) concentrations,[32] assuming 33% and 16% substitution of aluminum in each mineral, respectively.[33]

The organic carbon concentration was determined by the oxidation method using potassium dichromate (0.4 N). The P concentrations from the Mehlich-1 method (P_M) were determined using a double-acid extractant, 0.05 mol L^{-1} HCl + 0.0125 mol L^{-1} H_2SO_4. The remaining P (P_{rem}) was determined in the equilibrium solution after agitation of the soil samples (5 g) with a 0.01 mol L^{-1} $CaCl_2$ solution containing 60 mg kg^{-1} P. The P concentrations in the P_M and P_{rem} extracts were obtained by molecular absorption spectroscopy at 725 nm after the formation of the molybdenite-P complex via reduction by ascorbic acid (blue color).[34]

Vis-NIR spectra collection

All the spectra were collected using a FOSS NIRSystems XDS spectrometer (Silver Spring, MD, USA), which operates in the Vis-NIR region between the 400 and 2500 nm wavelengths.

Soil spectra

The soil samples (< 2 mm) were dried in an oven at 40 °C for 24 hours for standardization and reduction of the effect of moisture. An approximate mass sample of 5 g was scanned in a 50-mm diameter cylindrical cuvette with a quartz window. The spectral data were recorded in the reflectance mode to produce a spectrum with 1050 points and a spectral interval of 2 nm. Each sample spectrum represented an average of 32 readings. The average spectrum from three replicates for each layer of the soil profiles was obtained using the WinISI II v1.50 software (Foss NIRSystems/Tecator Infrasoft International, LLC, Silver Spring, MD, USA).

The results, expressed in absorbance (A), were obtained from the logarithm of the inverse of reflectance.

Spectra of the solutions

The same equipment was used to obtain the spectra of the P_M and P_{rem} sample solutions, which were collected using a solution volume of 15 mL in a 5-cm diameter glass cuvette with a height of 10 cm. Each sample spectrum represented an average of 32 readings. The average spectrum from three replicates for each solution was obtained using the WinISI II v1.50 software (Foss NIRSystems/Tecator Infrasoft International, LLC, Silver Spring, MD, USA). Hereafter, the term "solution" will be used to refer to the P_M and P_{rem} extraction solutions.

The reference standard for the physico-chemical relationship between P and the spectra was a 20 mg kg^{-1} monopotassium phosphate (KH_2PO_4) solution. These spectra were collected to observe the relationship between the reference spectra and those obtained for the soil P extraction solutions. For this purpose, the spectra of the solutions extracted from the soil samples from the 0.05 – 0.10 and 0.80 – 1.00 m layers of the profiles were used.

Pre-processing of the soil spectra

The pre-treatments applied to the spectra of the soil samples followed the recommendations of Brunet *et al.*[35] The derivatives were used to reduce the baseline variation and improve the visualization of the characteristic peaks of the spectra.[36,37] The first and second derivatives were calculated using four smoothing points and four points between gaps. This procedure was performed with or without the normalization of variances (SNV or SNVD) for the first and second derivative (144 and 244). The normalization procedure reduces the variation in the slope of a spectrum caused by the scattering effect and by variations in particle size[38,39] and it also removes the linear or curvilinear trend from a spectrum.[38] Thus, four pre-processing methods were used on the spectra: SNV 144, SNV 244, SNVD 144 and SNVD 244.

Principal component analysis (PCA) was performed on each sample from each data set (calibration, n=88; validation, n=177) and for each of the four pre-processing methods. The resulting principal components were used to determine the Mahalanobis (H) distance among the spectra and those with a distance greater than 3 were considered to be outliers and removed from the data set.[40]

Creation and calibration of the models

The two data sets (calibration and validation) were treated separately. The soil profile data set, n=88, was used for calibration and for the analysis of the relationships between the spectra and the two methodologies, P_M and P_{rem}. The set of samples from the surface layer, n=177, was used for model validation.

After elimination of the outliers, modified partial least squares regression (PLSRm) was used to correlate the spectral responses of the soils with the P_M and P_{rem} values. The cross validation of the calibration set (88 samples) was used to determine the optimal number of terms for the prediction model, as described in Barthès *et al.*[41] and Brunet *et al.*[35] and employed by Vendrame *et al.*[17] The calibration data bank was subdivided into eight groups, seven for model development and one to test the calibration. The calibration test was performed eight times. The residuals from the eight predictions were combined to calculate the standard error of the cross validation between the measured and predicted values (SECV). Samples with a residual 2.5-fold larger than the SECV were considered to be outliers (calibration outliers) and were removed from the databank. The subdivision procedure and analysis of the residuals were performed twice. All

of the samples in the calibration set were used to calculate the final model. The ideal number of factors of the calibration model was determined by the lowest SECV, and the efficiency of this model was evaluated using the coefficient of determination (R^2c) and the ratio of the standard deviation to the standard error of the cross validation (RPD). According to Viscarra Rossel *et al.*,[37] RPD values <1.0 indicate that the model is not suitable for prediction; RPD values between 1.0 and 1.4 indicate that the model may be used for prediction but only very disparate values can be differentiated; RPD values between 1.4 and 1.8 indicate a flawed prediction model, but the predicted values can be used for evaluation and correlation with other attributes; RPD values between 1.8 and 2.0 indicate a model that can be used for prediction and that quantitative analyses are possible; RPD values between 2.0 and 2.5 indicate a good model for quantitative analyses; finally, RPD values above 2.5 indicate an excellent prediction model for quantitative analyses.

The accuracy of the prediction and the validation of the models were determined by evaluating the R^2 validation value (R^2v), the standard error of prediction (SEP) and the correlation between the measured and predicted values.

Correlations between spectra and the P concentrations of the solutions and soil samples

An analysis of the Spearman's Rho correlation coefficients ($p<0.01$) between the spectra of the reference solution (KH_2PO_4) and the spectra of the P_M and P_{rem} solutions and the soil was made. This method was also used to evaluate the relationships of the spectra of the solutions with their P_{rem} and P_M concentrations.

The first derivative was used to determine the wavelengths that reflected the primary absorbance characteristics of the soil attributes. This result was associated with the loadings of the first vectors of the principal component. In addition to determining whether it can be used in the prediction of the attribute of interest, this relationship permits the verification of the result determined by the first derivative.

To analyze the influence of soil attributes on the spectra, the non-parametric Spearman's Rho correlations ($p<0.01$) between the wavelengths and the P_M and P_{rem} concentrations, and between the wavelengths and the concentrations of silicon, iron and aluminum oxides, organic matter, kaolinite, gibbsite, goethite and hematite were evaluated. The same method was used to analyze the correlations of the P_M and P_{rem} concentrations with the concentrations of organic matter, kaolinite, gibbsite, goethite, hematite and the ratio between the organic matter and iron oxide concentrations.

Due to the possibility of interference from organic carbon in determining the P_M concentrations,[20,21] the carbon concentration of 22 sample P_M solutions was determined using the Walkley & Black method,[42] using 3 mL of extract solution and following the principle of organic matter oxidation by $K_2Cr_2O_7$ (0.33 mol L^{-1}). From these results, a regression analysis of the relationship between the ratio of P and carbon (P/(P+C)) present in the solution and the P_M concentration in the soil was performed. The adopted model was selected based on the magnitude of the regression coefficient. The organic P concentrations (Po, mg kg^{-1}) were also calculated using the equation Po = 0.003C + 0.002, where C (g kg^{-1}) is the concentration of organic carbon.[43]

RESULTS

The soils

The means of the 17 soil attributes measured for the soil profiles and the surface samples are given in Table 1.

Table 1. Descriptive statistics of the clay concentration and chemical and mineralogical attributes of the latosol samples (n=265) from the calibration set (soil profiles, n=88) and validation set (surface soils, n=177)

Attributes	Average (±se[a])	Minimum	Median	Maximum
	Set 1 – Calibration (soil profiles n=88)			
Clay (g kg^{-1})	557 (±20.98)	234	586	880
SiO_2 (g kg^{-1})	124.3 (±4.49)	56.0	116.0	231.0
Al_2O_3 (g kg^{-1})	215.3 (±4.90)	126.0	225.0	285.0
Fe_2O_3 (g kg^{-1})	75.3 ±(2.99)	38.0	81.5	128.0
Kt[b] (g kg^{-1})	267.1 (±9.64)	120.2	249.1	496.1
Gb (g kg^{-1})	165.1 (±7.48)	71.9	156.5	341.4
Gt (g kg^{-1})	63.2 (±2.01)	32.6	63.6	100.2
Hm (g kg^{-1})	18.4 (±1.70)	2.6	10.6	67.1
R_{HG}	0.20 (±0.01)	0.06	0.19	0.50
R_{KGb}	0.62 (±0.02)	0.27	0.65	0.87
C (g kg^{-1})	16.41 (±1.08)	2.38	15.21	47.63
Ki	1.00 (±0.03)	0.37	1.04	1.62
Kr	0.83 (±0.03)	0.28	0.83	1.30
Po (mg kg^{-1})	5.12 (±0.32)	0.91	4.76	14.50
P_M (mg kg^{-1})	5.49 (±0.92)	0.45	1.50	42.02
P_{rem} (mg kg^{-1})	13.40 (±0.87)	1.57	12.33	38.62
	Set 2 – Validation (surface soils, n=177)			
Clay (g kg^{-1})	607 (±15.10)	210	656	899
SiO_2 (g kg^{-1})	200.89 (±6.76)	40.0	196.0	371.0
Al_2O_3 (g kg^{-1})	279.57 (±6.33)	125.0	298.0	455.0
Fe_2O_3 (g kg^{-1})	89.63 (±3.08)	17.0	104.0	164.0
Kt (g kg^{-1})	431.49 (±14.52)	85.9	421.0	796.8
Gb (g kg^{-1})	166.94 (±4.83)	52.3	152.7	401.2
Gt (g kg^{-1})	56.35 (±2.00)	0.0	54.2	139.0
Hm (g kg^{-1})	39.22 (±1.98)	0.0	43.8	154.0
RHG	0.39 (±0.01)	0.00	0.43	1.00
RCG	0.69 (±0.01)	0.30	0.71	0.91
C (g kg^{-1})	27.94 (±0.58)	14.07	27.41	49.26
Ki	1.18 (±0.02)	0.42	1.20	1.71
Kr	0.99 (±0.02)	0.35	1.02	1.49
P_M (mg kg^{-1})	11.53 (±0.39)	3.44	10.73	26.52
P_{rem} (mg kg^{-1})	19.12 (±0.56)	5.35	17.06	41.02

[a]se, standard error, [b]Kt, kaolinite, Gb, gibbsite, Gt, goethite, Hm, hematite, R_{KGb}, kaolinite and gibbsite ratio, R_{HG}, hematite and goethite ratio, C, organic carbon, Po, organic phosphorus, P_M, phosphorus extracted with Mehlich-1 and P_{rem}, remaining phosphorus.

Qualitative analysis of the spectra from the profile samples

Solution spectra

The reference solution (KH_2PO_4) spectrum contained a peak between 900 and 1100 nm. The peaks observed in the spectra of the P_M and P_{rem} solutions both exhibited a unique spectral pattern that was independent of the method of P acquisition, depth of collection and soil mineralogy, with a similar form to that of the reference solution (Figure 1Sa, b and c and Table 2).

Between the wavelengths from 900 to 1100 nm, the spectra had

Table 2. Correlation coefficients between the spectra of the reference solution, KH_2PO_4, and the spectra of the solutions resulting from the extractions of P_M and P_{rem} from the Latosols, with mineralogy varying from kaolinitic (Kt) to Oxidic, from the 0.05 – 0.10 and 0.80 – 1.00 m layers (n=3)

	P_M			P_M			P_{rem}			P_{rem}		
Layer	0.05-0.10 m			0.80-1.00 m			0.05-0.10 m			0.80-1.00 m		
Mineralogy	Kt	Kt-Oxidic	Oxidic-Gb	Kt	Kt-Oxidic	Oxidic-Gb	Kt	Kt-Oxidic	Oxidic	Kt	Kt-Oxidic	Oxidic
KH_2PO_4	0.98**	0.98**	0.98**	0.97**	0.97**	0.97**	0.97**	0.97**	0.97**	0.97**	0.96**	0.97**

**indicates a correlation value with p<0.01.

a significant and negative correlation (close to -0.80**) with the P_M concentrations of the soils. The correlation of this same spectral region with the P_{rem} concentrations was close to zero (Figure 1a).

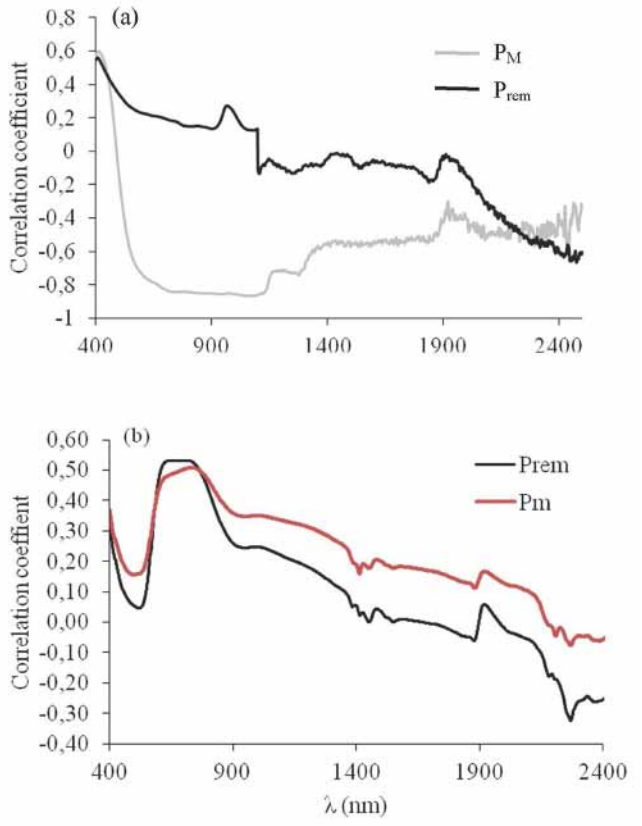

Figure 1. *Correlation coefficients of the concentrations of P Mehlich-1 (P_M) and P remaining phosphate (P_{rem}) of the soils with the spectra of their respective solutions (a) and with the soil spectra (b)*

The soil P_M concentrations were positively correlated with the concentrations of organic matter in the soils (Table 3). The P_M solutions from the 0.05 – 0.10 and 0.80 – 1.00 m layers of the soil profiles contained 0.10 to 0.40 mg mL^{-1} of carbon (mean 0.25 mg mL^{1}). There was no direct correlation between the organic carbon concentration of the P_M solution and the P_M concentration of the soil; however, for a given P concentration of the solution: the greater the extraction of C by the double acid solution, the greater the P_M concentration determined by colorimetry (Figure 2). The P_{rem} concentration was

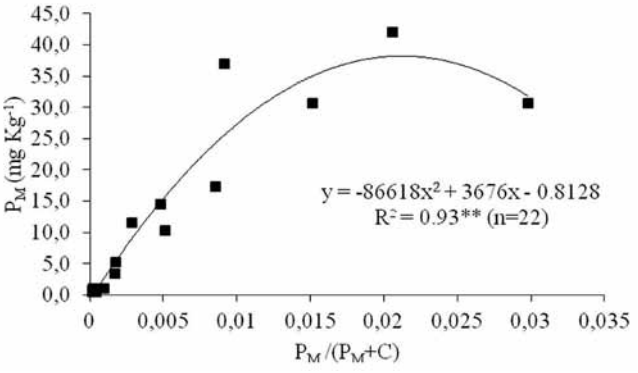

Figure 2. *Concentrations of phosphates extracted by the Mehlich-1 method plotted against the ratio of phosphate to organic carbon present in the extracts from the 0.05 – 0.10 m and 0.80 – 1.00 m layers of the 11 soil profiles*

correlated with the concentrations of clay and oxides, primarily hematite and aluminum oxide (Table 3).

Soil spectra

The spectra of the soil samples from the profiles contained five absorption peaks: between 400 and 550 nm, 750 and 1000 nm, 1350 and 1450 nm, 1850 and 2000 nm and 2120 and 2200 nm, as well as a region of high reflectance between 2200 and 2300 nm (see in Oliveira *et al.*).[28]

The spectrally active regions of the soil samples used to predict the P_M and P_{rem} concentrations were located in the region close to 550 nm in the visible range and in the regions of 1400 nm and from 2200 – 2300 nm in the near infrared. A region with a less-defined peak between 900 and 1100 nm was also observed (Figure 2S). For this last region, there is a negative correlation between the spectra of the P_M extraction solutions of the soil and the soil spectra (-0.42, p<0.01). This correlation was not observed for P_{rem}.

The P_M and P_{rem} concentrations were positively correlated with the spectra for the range between 600 and 810 nm, while the correlation coefficients for the region between 900 and 1100 nm were greater for P_M (r^2 between 0.30 and 0.40 (p<0.01)) than for P_{rem} (r^2 close to 0.20 (ns)) (Figure 1b).

PLSRm, modeling and prediction

Of the four pre-treatment methods performed on the soil spectra from the soil profiles, those with the first derivative (144) provided the best calibration results. The P_M concentrations had the lowest error

Table 3. Correlations of the P_M and P_{rem} concentrations with the clay, mineralogy and organic carbon contents of the soil (n=265)

	SiO_2	Al_2O_3	Fe_2O_3	Kt	Gb	Gt	Hm	Clay	R_{HG}	R_{KGb}	MO
P_M	0.03	-0.05	-0.19**	0.03	-0.16**	-0.23**	-0.09	-0.22**	0.03	0.079	0.41**
P_{rem}	-0.33**	-0.46**	-0.54**	-0.33**	-0.30**	-0.44**	-0.41**	-0.61**	-0.21**	-0.12	0.039

**indicates a correlation value with p<0.01.

Table 4. Results from the calibration and validation for the Mehlich-1 phosphorus concentration (P_M) and the remaining phosphorus concentration (P_{rem}) according to the pre-treatment method of the spectra (first and second derivative, 144 and 244, with and without removal of the trend, SVN and SNVD)

Attribute	Pre-processing method	Calibration Set				Validation Set			
		n_1	SECV (mg kg^{-1})	R^2c	RPD	n_2	SEP (mg kg^{-1})	R^2v	CV (%)
P_M	SNV 144	77	1.14	0.76	1.61	171	6.06	0.18	0.53
	SNV 244	80	1.55	0.60	1.15	171	5.40	0.12	0.47
	SNVD 144	78	1.15	0.75	1.38	170	7.92	0.10	0.69
	SNVD 244	80	1.52	0.65	1.30	171	5.20	0.15	0.45
P_{rem}	SNV 144	85	2.33	0.94	3.33	171	11.25	0.43	0.52
	SNV 244	87	2.62	0.94	3.88	171	8.50	0.49	0.52
	SNVD 144	86	2.36	0.93	3.54	170	7.73	0.48	0.52
	SNVD 244	87	2.61	0.94	3.89	171	8.95	0.48	0.52

values for the cross validation (SECV) and the highest coefficients of determination (R^2c) and RPD. For P_{rem}, the first derivative provided the lowest SECV (Table 4), despite producing similar values of R^2c and RPD relative to the second derivative (244).

Of the models developed for P_M, RPD values between 1.4 and 1.8 were observed only after the application of the SNV 144 pre-treatment, while values below 1.4 were observed for the other pre-treatments. The four models developed for P_{rem} produced RPD values greater than 2.5. Thus, for the analyses of correlations with the soil attributes, the SNV 144 model was used for P_M and the SNVD 144 model was used for P_{rem} because it had the lowest error prediction (SEP) (Table 4).

The first three principal components from the PLSRm of the P_M (SNV 144) and P_{rem} (SNVD 144) results explained more than 90% of the variance of the information contained in the spectra. The wavelengths observed in the first derivative (Figure 2S) and the peak close to 1,900 nm were determined to be the most important for model construction (Figure 3a and b). In contrast, the reference wavelengths between 900 and 1100 nm were not relevant to the model construction for P_M and P_{rem}.

Figure 4a and 4b present the relationships between the measured values and those predicted by the cross validation of the PLSRm. In the cross validation of P_M, the residuals of the prediction increase as a function of the increase in the P_M concentration in the soil, primarily beginning at 8 mg kg^{-1}, and the model is characterized by an R^2v of less than 0.2, regardless of the pre-treatment (Table 4 and Figure 4a). The P_{rem} model (SNVD 144) had an $R^2c = 0.93$; however, it was not suitable for the prediction of the soil P_{rem} concentrations, $R^2v = 0.48$ (Table 4 and Figure 4c).

The P_M and P_{rem} concentrations were positively and significantly correlated with the spectra for the wavelengths between 450 and 600 nm. P_M was also positively and significantly correlated with the spectra for the wavelengths between 900 and 1100 nm (Figure 1b). The reflectance at these wavelengths is primarily related to the concentrations of gibbsite, hematite and organic matter as well as the ratio between organic matter and iron (Figure 3S). In turn, P_{rem} was negatively and significantly correlated with the spectra for the peak between 2200-2300 nm (Figure 1b); this spectral region is related to the concentrations of clay, aluminum oxides[28] and goethite (Figure 3S).

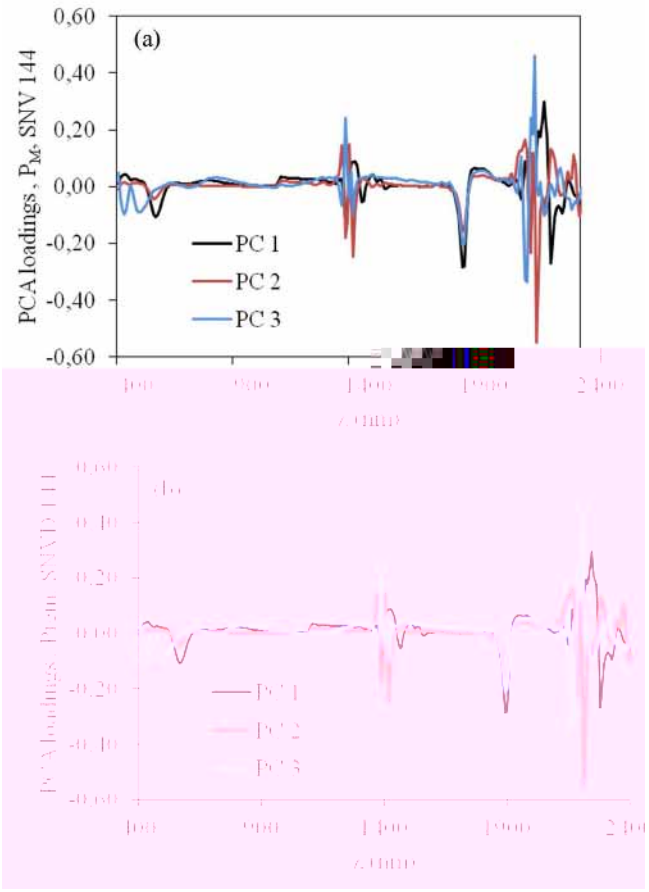

Figure 3. *Loadings of the principal components decoupled from the PLSRm of the SNV 144 model for P_M (a) and the SNVD 144 model for P_{rem} (b)*

DISCUSSION

Samples from the soil profiles

The texture of the soil profile samples varied from average to very clayey, with iron concentrations ranging between 50 and 250 g kg^{-1}, thus classifying them as hypo- to meso-ferric. The soils had kaolinitic, kaolinitic-oxidic and oxidic mineralogies (Table 1).[29] The mineralogical variation of these latosols can be explained by the influence of the local relief.[44,45]

The same level of variation in particle size, mineralogy and organic carbon of latosols was also observed by Balbino *et al.*[46] and Reatto *et al.*[45] for regional catenas from the Brazilian Central Plateau.

Spectra and concentrations of P_M and P_{rem} in the soils

Spectra from the P_M and P_{rem} phosphate extraction solutions

The spectrum of the reference solution (KH_2PO_4) contained an absorption peak between 900 and 1100 nm (Figure 1Sa). The spectra

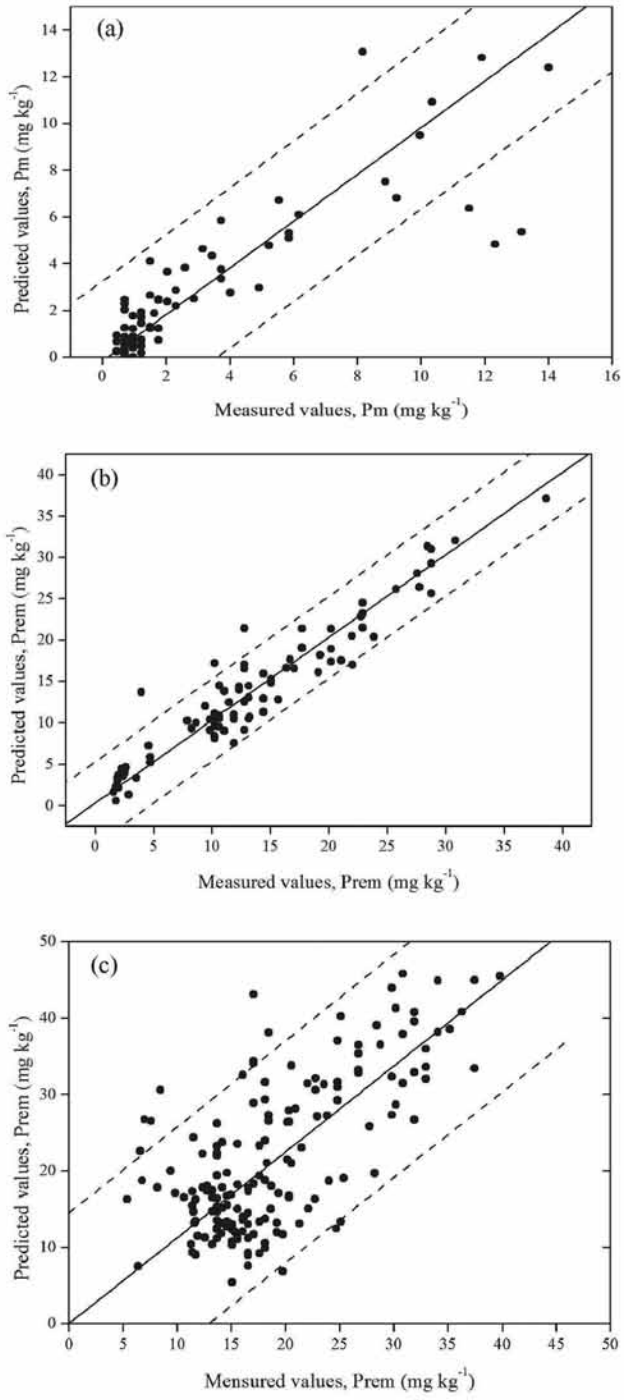

Figure 4. *Measured versus predicted values for the cross validation (PLSRm) of the model calibration with the SNV 144 pre-treatment for P_M (a; R^2c = 0.76; n = 77) (a), SNVD 144 for P_{rem} (b; R^2c = 0.93; n = 87) (b) and measured versus predicted values of P_{rem} obtained from the SNVD 144 model (R^2v = 0.48) (c). The dashed lines indicate the 95% confidence intervals for the predicted values*

of the P_M and P_{rem} solutions contained a similar absorption peak (Figure 1S b and c). This peak reflects the stretching frequency of the P-OH bond in association with the presence of non-polar, divalent or trivalent orthophosphate molecules in the solution.[4,8] Bogrekci and Lee[9] observed a maximum absorption of P_M in the region close to 900 nm in sandy soils incubated with different concentrations of P in the form of KH_2PO_4, and Maleki *et al.*[47] identified the wavelengths of 1003, 1009, 1103 and 1128 nm as the main peaks of Olsen-P observed in the Vis-NIR spectrum. Therefore, the P_M and P_{rem} solutions had functional P-OH groups from orthophosphate with characterization potential for P_M and P_{rem} by diffuse Vis-NIR reflectance spectroscopy. The similarity in the absorption spectra from the P_M and P_{rem} solutions, regardless of the depth, mineralogy and method, can be attributed to the light absorption properties of the water molecule, which homogenized the absorption intensity for the different concentrations of P in the solutions.[10]

The P concentrations of the P_M solution were negatively correlated (< -0.80, $p<0.01$) with the spectra for the wavelengths between 650 and 1150 nm (Figure 1a). This relationship is explained by the P-OH groups' (i.e. orthophosphate) present in the soil extracts and, also, by the extraction of organic carbon from the soil by the double-acid extractant used for P_M, as this region of the spectrum corresponds to the region of the third overtone of the C-H, $C-H_2$ and $C-H_3$ molecules.[3,16,48] This was observed with a significant correlation between the C and P_M concentrations of the soil samples (r^2=0.412**). For a given P concentration, the P_M concentration determined by colorimetry increases with an increase in the amount of C extracted by the double-acid solution (Figure 2). Organic carbon is solubilized by the Mehlich-1 method by an effect of the pH, the reaction of ions present in the extractant with the adsorbed molecules and, especially, the relationship between the mineral and organic forms of P.[49-51]

Considering the organic phosphorus, the samples from the soil profiles had Po concentrations between 0.91 and 14.50 mg kg^{-1} (Table 1), which, according to Chapuis-Lardy *et al.*,[43] may represent up to 75% of the total P present in latosols from the Brazilian Central Plateau and, according to Cross and Schlesinger,[52] up to 80% of the labile P of the latosols. This P fraction is primarily composed of the phosphates of sugars, monoesters, diesters, inositols and mononucleotides[21] and can be solubilized by the double-acid extractant used for P_M, as observed in Figure 2 and Table 3. The solubilization of Po by the double-acid extractant also explains the absence of a correlation between P_M and the aluminum oxide content and the weak relationship with the iron concentrations from the sulfuric acid extraction (Table 3).

The negative correlation between the P_M concentrations and the wavelengths between 650 and 1150 nm can be explained, in part, also by the formation of the molybdenic-P complex. The reaction between the P-monoester with molybdenum (which has an octahedral molecular structure) forms a tetrahedral molybdenum-P structure with lower absorbance energy. Thus, with an increase in the concentration of P determined by the molecular absorption method, the absorbance energy of the sample in the Vis-NIR region decreases.

The P_{rem} methodology evaluates the capacity for phosphate exchange between the solid soil phase and a calcium chloride solution initially containing 60 mg L^{-1} P. Thus, the absence of a correlation between the P_{rem} concentration and the wavelengths between 900 and 1100 nm can be explained by the presence of Ca^{2+} ($CaCl_2$) because it can precipitate the phosphate from the solution.[53] There is also the possibility of the formation of various layers of P around Ca by the action of Van der Waals forces, hindering the observation of a correlation between the P_{rem} concentration and the P_{rem} solution spectra.

Spectra of the soil samples

For the spectra of the soil samples, the region from 450 – 550 nm, those close to 1400 nm and 1900 nm, and that from 2200 – 2300 nm exhibited potential for the prediction of P_M and P_{rem}. In contrast, the region between 780 and 1000 nm had low absorption intensity with a poorly defined peak (Figures 2Sb). These results demonstrate that the physico-chemical relationship of the soil spectra with the P_M and P_{rem} concentrations is dependent on other soil attributes, without a specific molecular relationship, as observed for the spectra of the solution. This relationship was also observed by Daasch and Smith,[8]

Murray and Williams[4] and Bogrekci and Lee[9] when examining specific functional groups in aqueous media, prepared in the laboratory without interference from other soil attributes.

The regions from 450 550, 780 1100 and close to 2200 nm can be spectrally active for the prediction of P_M concentrations because of the interaction of P with the organic matter of the soil. In this regard, the regions between 450 and 630 and between 680 and 800 nm are sensitive to the different stages of decomposition and the origin of the organic matter;[54] the region between 780 and 1100 nm contains peaks that are characteristic of polysaccharides;[55,56] the region close to 2200 nm contains absorption peaks that are associated with the elementary vibration of the P bound to hydrocarbons or to phenyl rings.[8]

The regions between 450 and 550, 780 and 1100, and 2200 and 2300 nm can be spectrally active for the prediction of P_{rem} because of the relationships of these regions of the spectrum to the soil mineralogy.[26,28] P_{rem} was indirectly correlated with the spectrum of the soil because of its adsorption to iron oxides (goethite) and aluminum oxides (gibbsite) (Table 3 and Figure 3b). The iron oxides promoted an absorption peak in the region between 450 and 550 nm that is associated with the trivalent iron ions and those bound to hydroxyl groups.[57-59] The aluminum oxides promoted a peak in the regions between 900 and 1100 nm and between 2200 and 2300 nm in association with the vibrations caused by the stretching of the OH groups present in gibbsite.[26,55,56]

The peaks at 1400 and 1900 nm may have a direct relationship with the P_M and P_{rem} of the soil that is associated with the stretching bands of R-OH,[3,60] which may be represented by P-OH in the P_M and P_{rem} solutions. Additionally, Daasch and Smith[8] have noted that this region of the spectrum may also contain peaks that are characteristics of the essential vibrations caused by the stretching of P-H bonds.

The results indicate that Vis-NIR measurements can be used to construct models for the prediction of P_M concentrations, given that the reference region between 900 and 1100 nm also characterizes the P_M of the solution and is shown to be active in the soil spectra. The construction of models for the prediction of P_{rem} concentrations must be viewed with caution because the P_{rem} concentrations were correlated with the wavelengths between 450 and 550 nm and between 2200 and 2300 nm of the soil spectra, which were strongly influenced by the mineralogy and were not correlated with the spectral regions of the reference solution or that used in the colorimetric method.

Construction of the models

Four pre-treatments were applied to the soil spectra for correction of light scattering (SNV 144, SNV 244, SNVD 144 and SNVD 244). The best calibration results were obtained with the models that used the first derivative (SNV 144 and SNVD 144) which characterizes the absorption peaks, with a negative value when the absorption decreases and a positive value when it increases. In turn, the second derivative uses the absorbance minimum of the sample in the calculation, emphasizing only the most characteristic peaks present in the spectra, which correspond to the primary parameters (molecules of C, N, H and O). Thus, the use of the second derivative decreases the sensitivity of Vis-NIR in detecting secondary parameters and thus P.

The calibration model for P_M (SNV 144) had an RPD value of 1.61, indicating that it can only be used for analysis of the relationships of this P fraction with other soil attributes. The P_{rem} calibration model (SNVD144), with an RPD value > 2.5, could be used for qualitative and quantitative analyses; however, despite the excellent calibration quality, the validation was not satisfactory (Table 4).

The unsatisfactory validation of the P_{rem} model was likely associated with the superposition of peaks from the same region of the spectrum. The interval between 450 and 550 nm is related to the OM/Fe_2O_3 ratio. The regions close to 1400 and 1900 nm and the interval between 2200-2300 nm are related to iron and aluminum oxides, notably hematite and gibbsite, respectively. The reference region, 900 to 1100 nm, is related to organic carbon ($R^2 > 0.40$**) (Figure 3S).

This superposition of peaks explains the validation error of the SNV 144 model for P_M, especially for samples with more than 8 mg P kg^{-1}, given that spectra from the soil in the region between 450 and 550 and in the reference region (between 900 and 1100 nm) are related to the OM/Fe_2O_3 ratio and organic matter, respectively. Thus, the observed peaks in the P_M spectra could be associated with a specific adsorption site or weakly associated to the surface of polysaccharides or other organic compounds.[22,24,25,61,62] As a result there was no characteristic signal in the spectrum, confirming that the observed signal is not associated with mineralogy, as reported in Van Raij *et al.*,[48] Pozza *et al.*[24] and Eberhardt *et al.*[49] The validation was performed with samples from the surface layer. This layer is associated with the greatest physical-chemical complexity of P_M, which may negatively affect the model because this population was not represented in the calibration set.

The peaks in the region between 900 and 1100 nm of the soil spectra may be from hydroxyls bonded to alcohol molecules, ali-

This study demonstrated that Vis-NIR has the potential for studies that involve P in the soil, in orthophosphate form, especially for the region between 900 and 1100 nm. However, the methodology employed for the analysis of the secondary attributes of interest has an effect on the spectral response, potentially hindering the observation of relationships between the attribute of interest and the spectrum. Thus, methodologies must be considered that do not alter the physical-chemical characteristics of the samples, such as resin extraction methods for soil phosphate studies.

For the data set examined in this study, the complexity of the P dynamics in the soil and its relationship with the spectra can result in the generation of models that consist of a "mathematical coincidence", without necessarily having a physical-chemical foundation. Additionally, the spectra of the solution of determination does not have a direct relationship with the concentrations of this form of P in the soil and the regions of the soil spectrum that permit the prediction of P_{rem} are strongly influenced by its mineralogy.

Thus, the resumption of pre-processing as originally conceived, such as the removal of organic matter and amorphous iron oxides, could aid in the acquisition of better spectral results for determining soil phosphorus concentrations, especially when associated with its fractionation, but there is no direct relationship with the potentially bioavailable P.

CONCLUSIONS

The spectra of the P_M and P_{rem} solutions contained an absorption peak in the region between 900 and 1100 nm, similar to the reference spectrum, demonstrating the potential for the characterization of soil P_M and P_{rem} by diffuse Vis-NIR reflectance spectroscopy.

In the soil spectra, the regions that were active for the prediction of P_M and P_{rem} differed from those that were observed in the reference solution (KH_2PO_4), the P_M extraction solution and the P_{rem} determination solution, with absorption peaks between 450 and 550 nm, close to 1400 and 1900 nm, and between 2200 and 2300 nm. The region between 780 and 1000 nm had a low absorption intensity with a poorly defined peak, demonstrating that the physical-chemical relationship of the soil spectra with the P_M and P_{rem} concentrations is dependent on other soil attributes.

The P_M prediction models for quantitative analyses, especially in samples with more than 8 mg P kg^{-1}, is hindered by extraction of organic matter by the double-acid extractant and the correlations of the soil spectra at the wavelengths between 450 and 550 and between 900 and 1100 nm with the OM/Fe_2O_3 ratio and organic matter content, respectively.

Despite the RPD values > 2.5 found in the calibration, the use of the models for the prediction of P_{rem} in the surface layers of the latosols must be viewed with caution because the P_{rem} concentrations were positively correlated with the spectra for the wavelengths between 450 and 550 nm and between 2200 and 2300 nm and these regions are strongly influenced by mineralogy, primarily the presence of iron and aluminum oxides in the form of goethite and gibbsite, respectively, and not correlated with the spectral regions of greatest reflectance in the reference solutions or that used in the colorimetric method.

SUPPLEMENTARY MATERIAL

Figure 1S a and b: supplementary previously published by Oliveira *et al.*,[28]

Figure 2S: correlation coefficient between soil attributes and wavelengths 400 – 2500 nm.

Figures 1S and 2S are available at http://quimicanova.sbq.org.br with free access.

REFERENCES

1. White, J. L.; Roth, C. B. In *Methods of Soil Analysis, Part. I: Physical and Mineralogical Methods*, 2nd ed.; Campbell, G. S.; Jackson, R. D.; Mortland, M. M.; Nielsen, D. R.; Klute, A., eds.; American Society of Agronomy and Soil Science Society of America: Madison, WI, 1986, pp. 291-329.
2. Stenberg, B.; Viscarra Rossel, R. A.; Mouazen, A. M.; Wetterlind, J. *Visible and Near Infrared Spectroscopy in Soil Science*. In *Advances in Agronomy, Vol. 107*; Sparks, D. L., ed.; Academic Press: London, UK, 2010, chap. 5.
3. Xiaobo, Z.; Jiewen, Z.; Povey, M. J. W.; Holmes, M.; Hanpin, M.; *Anal. Chim. Acta* **2010**, *667*, 14.
4. Murray, I.; Williams, P. C. In *Near-Infrared Technology in the Agricultural and Food Industries*; Williams, P. C.; Norris, K. H., eds.; American Association of Cereal Chemists: St. Paul, MN, 1987, chap. 2.
5. Pasquini, C.; *J. Braz. Chem. Soc*. **2003**, *14*, 198.
6. Turner, B. L.; *J. Ecol*. **2008**, *96*, 698.
7. Wu, C. Y.; Jacobson, A. R.; Laba, M.; Kim, B.; Baveye, P. C.; *Water Air Soil Pollut*. **2010**, *209*, 377.
8. Daasch, L. W.; Smith, D. C.; *Anal. Chem*. **1951**, *23*, 853.
9. Bogrekci, I.; Lee, W. S.; *Biosystems Eng*. **2005**, *91*, 305.
10. Bogrekci, I.; Lee, W. S.; *Trans. ASABE* **2006**, *49*, 1175.
11. Maleki, M. R.; Mouazen, A. M.; Ramon, H.; De Baerdemaeker, J.; *Soil Tillage Res*. **2007**, *94*, 239.
12. Maleki, M. R.; Mouazen, A. M.; De Ketelaere, B.; Ramon, H.; De Mouazen, A. M.; Maleki, M. R.; De Baerdemaeker, J.; Ramon, H.; *Soil Tillage Res*. **2007**, *93*, 13.
13. Mouazen, A.M.; Maleki, M.R.; De Baerdemaeker, J. ; Ramon, H.; *Soil Tillage Res*. **2007**, *93*, *13–27*.
14. Lu, P.; Wang, L.; Niu, Z.; Li, L.; Zhang, W.; *J. Geochem. Explor*. **2013**, *132*, 26–33.
15. Vågen, T-G.; Shepherd, K. D.; Walsh, M. G.; *Geoderma* **2006**, *133*, 281.
16. Viscarra Rossel, R. A.; Walvoort, D. J. J.; Mcbratney, A. B.; Janik, L. J.; Skjemstad, J. O.; *Geoderma* **2006**, *131*, 59.
17. Vendrame, P. R. S.; Marchão, R. L.; Brunet, D.; Becquer, T.; *Eur. J. Soil Sci*. **2012**, *63*, 743.
18. Majed, N.; Li, Y.; Gu, A. Z.; *Curr. Opin. Biotechnol*. **2012**, *23*, 852.
19. Hedley M. J.; Mortvedt J. J.; Bolan N. S.; Syers J. K. In *Phosphorus in the Global Environment*; Tiessen, H., ed.; John Wiley & Sons: Chichester, 1995, chap. X.
20. Grande, M. A.; Curi, N.; Quaggio, J. A.; *Rev. Bras. Cienc. Solo* **1986**, *10*, 45.
21. Chapuis-Lardy, L.; Brossard, M.; Quiquampoix, H.; *Can. J. Soil Sci*. **2001**, *81*, 591.
22. Frossard, E.; Brossard, M.; Hedley, M; Metherell, A. In *Phosphorus in the Global Environment*. Tiessen, H., ed.; John Wiley & Sons: Chichester, 1995, chap. 7.
23. Brossard, M.; Chapuis-Lardy, L. C. *R.*; *Resumo do XVI Congresso Mundial de Ciência do solo*, Montpellier, França, 1998.
24. Pozza, A. A. A.; Curi, N.; Costa, E. T. S.; Guilherme, L. R. G.; Marques, J. J. G. S. M.; Motta, P. E. F.; *Pesq. Agropec. Bras*. **2007**, *42*, 1627.
25. Pozza, A. A. A.; Curi, N.; Guilherme, L. R. G.; Marques, J. J. G. S. M.; Costa, E. T. S.; Zuliani, D. Q.; Motta, P. E. F.; Martins, R. S.; Oliveira, L. C. A.; *Quim. Nova* **2009**, *32*, 99.
26. Madeira, J.; Bédidi, A.; Pouget, M.; Cervelle, B. E.; Flay, N.; *C. R. Acad. Sci. Paris* **1995**, *321*, 119.
27. Madeira, J., Beïdidi, A., Cervelle, B., Pouget, M.; Flay, N.; *Int. J. Remote Sens*. **1997**, *18*, 2835.
28. Oliveira, J. F.; Brossard, M.; Vendrame, P. R. S.; Mayi III, S.; Corazza, E. J.; Marchão, R. L.; Guimarães, M. F.; *C. R. Geosci*. **2013**, *345*, 446.
29. Santos, H. G.; Jacomine, P. K. T.; Anjos, L. H. C.; Oliveira, V. A.; Oliveira, J. B.; Coelho, M. R.; Lumbrelas, J. F.; Cunhas, T. J. F.; *Sistema*

Brasileiro de Classificação de Solos; Centro Nacional de Pesquisa de Solos: Rio de Janeiro, Brasil, 2006.
30. Claessen, M. E. C. In *Manual de Métodos de Análise de Solo*, 2nd ed., Embrapa-CNPS: Rio de Janeiro, 1997.
31. Resende, M.; Bahia Filho, A. F. C.; Braga, J. M.; *Rev. Bras. Cienc. Solo* **1987**, *11*, 17.
32. Resende, M.; Santana, D. P.; *Anais da 3. Reunião de Classificação, Correlação de Solos e Interpretação de Aptidão Agrícola*, EMBRAPA–SNLCS/SECS, Rio de Janeiro, 1988.
33. Schwertzmann, U.; Taylor, R. M. In *Minerals in Soil Environments*; Dixon, J. B.; Weed, S. B., eds.; Soil Science Society of America: Madison, 1989, chap. 8.
34. Donagema, G. K.; Campos, D. V. B.; Calderano, S. B.; Teixeira, W. G.; Viana, J. H. N. In *Manual de Métodos de Análise de Solos*, 2nd ed., Embrapa Solos: Rio de Janeiro, 2011.
35. Brunet, D.; Barthès, B. G.; Chotte, J. L.; Feller, C.; *Geoderma* **2007**, *139*, 106.
36. Reeves III, J. B.; McCarty, G. W.; Mimmo, T.; *Environ. Pollut.* **2002**, *116*, S277.
37. Viscarra Rossel, R. A.; Mcglynn, R. N.; Mcbratney, A. B.; *Geoderma* **2006**, *137*, 70.
38. Barnes, R. J.; Dhanoa, M. S.; Lister, S. J.; *Appl. Spectrosc*. **1989**, *43*, 772.
39. Candolfi, A.; De Maesschalck, R.; Jouan-Rimbaud, D.; Hailey, P. A.; Massart, D. L.; *J. Pharm. Biomed. Anal*. **1999**, *21*, 115.
40. Shenk, J. S.; Westerhaus, M. O.; *Crop Sci.* **1991**, *31*, 469.
41. Barthès, B. G.; Brunet, D.; Ferrer, H.; Chotte, J. L.; Feller, C.; *J. Near Infrared Spectrosc*. **2006**, *14*, 341.
42. Walkley, A.; Black, A.; *Soil Sci*. **1934**, *37*, 29.
43. Chapuis-Lardy, L.; Brossard, M.; Lopes Assad, M. L.; Laurent, J. Y.; *Agric. Ecosyst. Environ*. **2002**, *92*, 147.
44. Camargo, L. A.; Marques Júnior, J.; Pereira, G. T.; Horvat, R. A.; *Rev. Bras. Cienc. Solo* **2008**, *32*, 2279.
45. Reatto, A.; Bruand, A.; Martins, E. S.; Muller, F.; Silva, E. M.; Carvalho Jr, O. A.; Brossard, M.; *C. R. Geosci*. **2008**, *340*, 741.
46. Balbino, L. C.; Brossard, M.; Leprun, J.-C.; Bruand, A.; *Étude et Gestion des Sols* **2002**, *9*, 83.
47. Maleki, M. R.; Van Holm, L.; Ramon, H.; Merckx, R.; De Baerdemaeker, J.; Mouazen, A. M.; *Biosyst. Eng*. **2006**, *95*, 425.
48. Lima, K. M. G.; Raimundo Jr., I. M.; Silva, A. M. S.; Pimentel, M. F.; *Quim. Nova* **2009**, *32*, 1635.
49. Van Raij, B.; *Rev. Bras. Cienc. Solo* **1978**, *2*, 1.
50. Eberhardt, D. N.; Vendrame, P. R. S.; Becquer, T.; Guimarães, M. F.; *Rev. Bras. Cienc. Solo* **2008**, *32*, 1009.
51. Bortolon, L.; Gianello, C.; *Rev. Bras. Cienc. Solo* **2010**, *34*, 263.
52. Cross, A. F.; Schlesinger, W. H.; *Geoderma* **1995**, *64*, 197.
53. Rietra, R. P. J. J.; Hiemstra, T.; Van Riemsdijk, W. H.; *Geochim. Cosmochim. Acta* **1999**, *63*, 3009.
54. Ben-Dor, E.; Inbar, Y.; Chen, Y.; *Remote Sens. Environ*. **1997**, *61*, 1.
55. Castellano, M.; Turturro, A.; Riani, P.; Montanari, T.; Finocchio E.; Ramis G.; Busca G.; *Appl. Clay Sci*. **2010**, *48*, 446.
56. Tivet, F.; Sá, J. C. M.; Lal, R.; Milori, D. M. B. P.; Briedis, C.; Letourmy, P.; Pinheiro, L. A.; Borszowskei, P. R.; Hartman, D. C.; *Geoderma* **2013**, *207-208*, 71.
57. Hunt, G. R.; Salisbury, J. W.; Lenhoff, C. J.; *Mod. Geol*. **1971**, *2*, 195.
58. Hunt, G. R.; *Geophysics* **1977**, *42*, 501.
59. Lugassi, R.; Ben-Dor, E.; Eshel, G.; *Geoderma* **2014**, *213*, 268.
60. Hunt, G. R.; Hall, R. B.; *Clays Clay Miner*. **1981**, *29*, 76.
61. Fassbender, H. W. In *Quimica de Suelos com Énfasis em Suelos de América Latina*; Fassbender, H. W.; Bornemisza, E., eds.; Instituto Interamericano de Ciências Agrícolas: San Jose, 1978, chap. 10.
62. Bahia Filho, A. F. C.; Braga, J. M.; Resende, M.; Ribeiro, A. C.; *Rev. Bras. Cienc. Solo* **1983**, *7*, 221.
63. Dabin, B. In: *Soil related constraints to good production in the tropics*. Colloquium, Los Banos, 1980, p.217-232.
64. Donagema, G. K.; Ruiz, H. A.; Alvarez V. H.; Ker, J. C.; Fontes, M. P. F.; *Rev. Bras. Cien. Solo* **2008**, *32*, 1785.

VIS-NIR SPECTROMETRY, SOIL PHOSPHATE EXTRACTION METHODS AND INTERACTIONS OF SOIL ATTRIBUTES

José Francirlei de Oliveira[a], Michel Brossard[b], Edemar Joaquim Corazza[c], Robélio Leandro Marchão[d], Pedro Rodolfo Siqueira Vendrame[e], Osmar Rodrigues Brito[a] and Maria de Fátima Guimarães[a,*]

[a]Departamento de Agronomia, Centro de Ciências Agrárias, Universidade Estadual de Londrina, Rodovia Celso Garcia Cid, PR 445, Km 380, 86051-980 Londrina – PR, Brasil

[b]Institut de recherche pour le développement, UMR 210 Eco&Sols, BP 64501, 34394 Montpellier cedex 5, France

[c]Embrapa Informação Tecnológica, CP 040315, 70770-901 Brasília – DF, Brasil

[d]Embrapa Cerrados, CP 08223, 73310-970 Planaltina – DF, Brasil

[e]Departamento de Geociências, Universidade Estadual de Londrina, CP 6001, 86051-990 Londrina – PR, Brasil

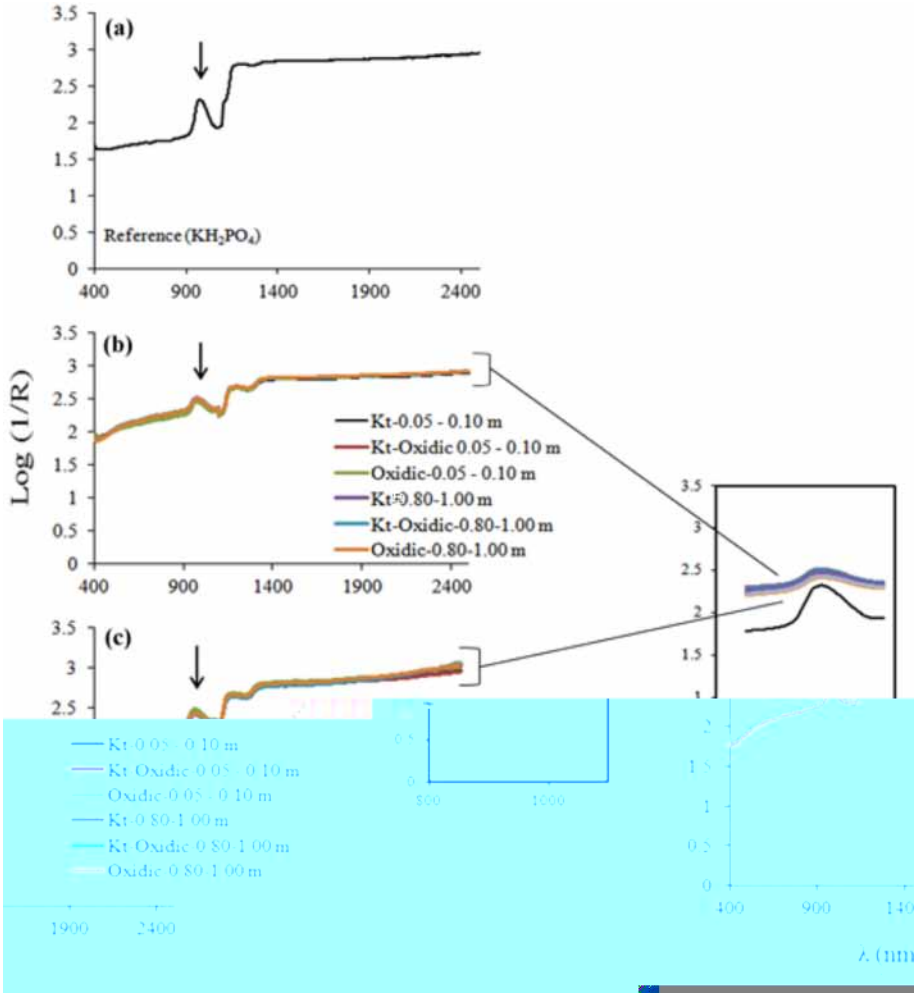

Figure 1S. *Diffuse Vis-NIR reflectance spectra for the reference solution (KH_2PO_4) (a), and for P_M solutions and (b) P_{rem} solutions (c) from the 0.05 – 0.10 and 0.80 – 1.00 m layers. Spectra for the reference, P_M and P_{rem} solutions for the region between 800 and 1100 nm (d). The spectra are shown as a function of the mineralogy of the samples, classified as kaolinitic (Kt), kaolinitic-oxidic (Kt-Oxidic) and oxidic*

*e-mail: mfatima@uel.br

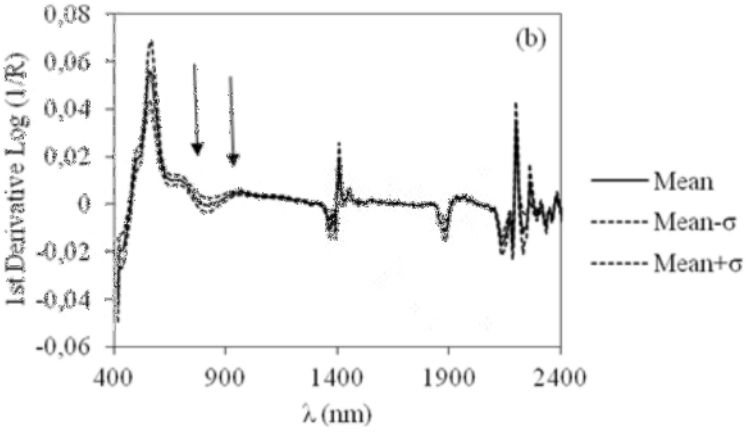

Figure 2S. *First derivative of the spectra of samples from the 11 soil profiles (n=88) used for model calibration*

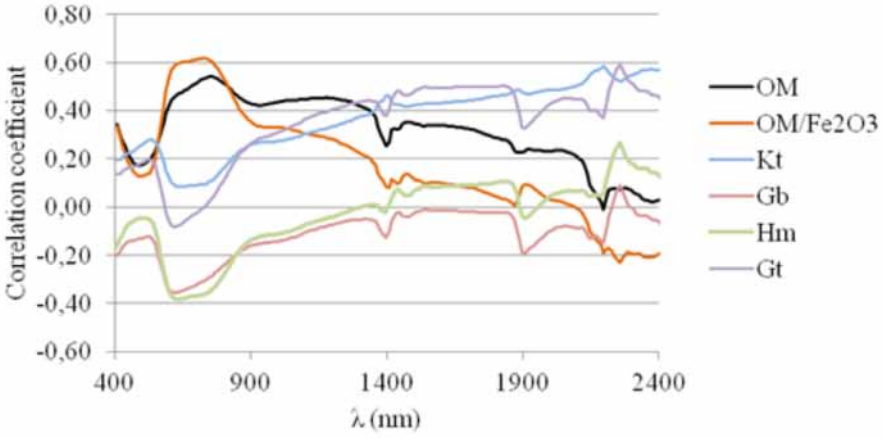

Figure 3S. *Correlation coefficients between the spectra and the organic matter to iron ratio, and the organic matter, kaolinite (Kt), gibbsite (Gb), goethite (Gt) and hematite (Hm) contents of the soil profile samples*